Ex Vivo Histological Characterization of a Novel Ablative Fractional Resurfacing Device

Basil M. Hantash, MD, PhD,[1,2] Vikramaditya P. Bedi, MS,[2] Kin Foong Chan, PhD,[2]* and Christopher B. Zachary, MBBS, FRCP[3]
[1]*Stanford University School of Medicine, Stanford, California 94305*
[2]*Reliant Technologies, Inc., Mountain View, California 94043*
[3]*University of California, Irvine, California 92697*

Background and Objectives: We introduce a novel CO_2 laser device that utilizes ablative fractional resurfacing for deep dermal tissue removal and characterize the resultant thermal effects in skin.
Study Design/Materials and Methods: A prototype 30 W, 10.6 μm CO_2 laser was focused to a $1/e^2$ spot size of 120 μm and pulse duration up to 0.7 milliseconds to achieve a microarray pattern in ex vivo human skin. Lesion depth and width were assessed histologically using either hematoxylin & eosin (H&E) or lactate dehyrdogenase (LDH) stain. Pulse energies were varied to determine their effect on lesion dimensions.
Results: Microarrays of ablative and thermal injury were created in fresh ex vivo human skin irradiated with the prototype CO_2 laser device. Zones of tissue ablation were surrounded by areas of tissue coagulation spanning the epidermis and part of the dermis. A thin condensed lining on the interior wall of the lesion cavity was observed consistent with eschar formation. At 23.3 mJ, the lesion width was approximately 350 μm and depth 1 mm. In this configuration, the cavities were spaced approximately 500 μm apart and interlesional epidermis and dermis demonstrated viable tissue by LDH staining.
Conclusion: A novel prototype ablative CO_2 laser device operating in a fractional mode was developed and its resultant thermal effects in human abdominal tissue were characterized. We discovered that controlled microarray patterns could be deposited in skin with variable depths of dermal tissue ablation depending on the treatment pulse energy. This is the first report to characterize the successful use of ablative fractional resurfacing as a potential approach to dermatological treatment. Lasers Surg. Med.

Key words: ablation; infrared lasers; CO_2; collagen; fractional photothermolysis; MTZ

INTRODUCTION

Resurfacing of photoaged facial skin with ablative lasers represents a significant advance as a method of rejuvenation [1]. Numerous studies have clearly demonstrated the clinical efficacy of this treatment modality using infrared laser sources such as CO_2 or Erbium:YAG [2–5]. However, these treatment modalities suffer from side effects such as prolonged post-treatment downtime, post-inflammatory pigmentary alterations, persistent erythema, edema, infection, and scarring [1,6–8]. Hence ablative laser resurfacing, once the mainstay of skin rejuvenation, has been significantly less popular in recent years. This has led many laser surgeons to switch to less invasive treatment modalities such as non-ablative laser rejuvenation in an attempt to minimize risk to patients.

Although non-ablative laser treatment has delivered increased clinical safety, this has often come at a cost of predictable and consistent efficacy [9,10]. More recently, a major advance in non-ablative laser treatment, termed fractional photothermolysis, was reported [11]. In this critical study, re-epithelialization was achieved in 24 hours, thus reducing patient downtime significantly. Our group demonstrated that a novel non-ablative fractional resurfacing modality with discreet epidermal and dermal lesions, coined microscopic treatment zones (MTZ), could be created using a mid-infrared laser emitting at 1.5 μm wavelength, while sparing the surrounding tissue [12]. Thus, only 20–35% of skin surface cross-sectional area would be treated in any one session rather than inducing a homogenous thermal injury of 100% of the target skin. In three-dimensional terms, the percentage volumetric coverage in fractional resurfacing can be increased by treatments at higher pulse energies to achieve deeper micro-lesions. Since the introduction of this nonablative fractional resurfacing modality, numerous investigators have confirmed both its safety as well as its efficacy for indications such as melasma, acneiform scarring, and non-facial skin photorejuvenation [13–16]. Indeed, Fisher et al. [13] reported only transient side effects lasting 3–7 days post treatment and the complete absence of more serious adverse events such as pigmentary alteration, herpetic activation, persistent erythema or edema, and infection; all commonly seen with ablative laser resurfacing. Although the average pain score was 4.6 on a scale of 10, another study by the same investigators revealed a 40% reduction of pain scores with

*Correspondence to: Dr. Kin F. Chan, Reliant Technologies, Inc., 464 Ellis Street, Mountain View, CA 94043.
E-mail: kchan@reliant-tech.com
K.F.C. has disclosed a potential financial conflict of interest with this study.
Accepted 4 August 2006
Published online in Wiley InterScience (www.interscience.wiley.com).
DOI 10.1002/lsm.20405

concurrent use of a handheld forced cold air device [17]. Furthermore, pain scores varied depending on location and intensity of treatment with average pain scores of 3.2 on a scale of 10 reported in the periorbital region [11].

Although the clinical photorejuvenation effects of non-ablative fractional resurfacing are unquestionable, the efficacy for the treatment of rhytides remains to be determined. Thus far, modest results have been demonstrated in treatment of periorbital rhytides with a 2.1% linear shrinkage at 3 months after therapy [11]. These results were achieved after four treatments (6–12 mJ; 2,500 MTZ per cm^2) spaced 2–3 weeks apart. It remains unclear how variations in pulse energy will influence the efficacy of rhytides treatment.

To overcome some of the ongoing limitations, we decided to explore the combination of ablative laser resurfacing and fractional resurfacing. We surmised that the concept of tissue sparing may allow improved efficacy over non-ablative lasers while minimizing the typical troubling side effects of ablative laser resurfacing treatment. By focusing ablative laser beams to microscopic spot sizes and delivering them with a fractional approach, the removal of deep dermal tissue not possible with conventional ablative laser resurfacing may produce efficacious deep dermal remodeling while promoting rapid epidermal wound healing. The use of this laser configuration to treat human skin in vivo may offer improvements in tissue shrinkage and skin tightening when compared to non-ablative infrared lasers as well as reduced patient downtime relative to current ablative laser devices. Thus, we believe the adaptation of a novel ablative fractional resurfacing modality with a hemostatic far-infrared laser may represent a revolutionary future approach to photorejuvenation.

In this report, we characterize the lesion dimensions in human ex vivo skin treated with a far-infrared CO_2 laser emitting at 10.6 μm wavelength. We show for the first time that controlled MTZ of injury can be created with variable depths and widths that correlate with pulse energy. Similar to the 1.5 μm wavelength fiber laser, the CO_2 laser configured to deliver in a microscopic spot-array pattern can result in significant sparing of both epidermal and dermal tissues because of the fractional approach.

METHODS

Freshly excised human abdominal skin samples (Fitzpatrick skin type II) were irradiated with a 30 W, 10.6 μm CO_2 (AFR^{TM}) laser (Reliant Technologies, Inc., Mountain View, CA) in order to investigate the effects on ex vivo human skin and determine the dimensions of individual lesions at varying pulse energies. The laser beams carried a near diffraction limited $1/e^2$ Gaussian spot size of approximately 120 μm, with pulse energies ranging from 8 to 20 mJ that were delivered through a new prototype capable of a repetition rate up to 1,500 spots/second.

Prior to laser treatment, the subcutaneous fat was trimmed and hair shaved from each skin sample. After cutting to a size of 15×70 mm, the skin was placed between two saline soaked $4'' \times 4''$ gauze pads and heated on a digital hot plate (Cole-Parmer Instrument Co., Vernon Hills, IL). The skin surface temperature was measured with a Mintemp MT4 infrared probe (Raytek Corporation, Santa Cruz, CA), and laser treatment initiated once reaching $98 \pm 3^{\circ}F$. Immediately prior to treatment, the top layer of gauze was removed and the lower gauze and tissue sample were transferred to an aluminum hot plate set at $98^{\circ}F$. The laser handpiece was translated at a specific velocity by using a precision linear stage driven by an ESP 300 motion controller (Newport Co., Irvine, CA). The firing rate of the laser was automatically adjusted by the laser handpiece to produce a specific density of lesions [18]. In the pulse energy range of 8–20 mJ, we encountered a $17 \pm 4\%$ discrepancy between set (value on user interface) and measured pulse energy. These offsets were accounted for in our measurements and calculations. A single pass was made at a constant velocity of 1.0 cm/second and spot density of 400 MTZ/cm^2 creating an interlesional distance of approximately 500 μm.

Samples were then cut into smaller specimens and then either embedded in optimal cutting temperature compound (IMEB, Inc., San Marcos, CA) and frozen sectioned, or fixed in 10% v/v neutral buffered formalin (VWR International, West Chester, PA) and paraffin sectioned, using either vertical or horizontal slices 5–15 μm or 10–20 μm thick, respectively, and stained with LDH or H&E. Stained samples were imaged using a DM LM/P microscope and a DFC320 digital camera (Leica Microsystem, Cambridge, UK). The lesion dimensions were measured with a proprietary Visual Basic computer program (Reliant Technologies, Inc.) [18]. The lesion dimension represents the maximum depth and width of the ablated cavity plus the outermost border of the coagulation or viability zone histologically determined by H&E or LDH staining, respectively.

RESULTS

This novel AFR^{TM} prototype CO_2 laser created a pattern of microscopic spots separated by viable normal tissue in freshly isolated ex vivo abdominal tissue. H&E and LDH staining patterns of irradiated tissue are demonstrated in Figures 1 and 2, respectively. Each figure illustrates the creation of a tapering cavity lined by a thin layer of eschar formation, consistent with an ablative laser treatment. The eschar formation was itself surrounded by an annular zone of thermal coagulation representing denatured collagen. This was demonstrated by hyalinization or loss of birefringence under cross-polarized microscopy in H&E stained panels. Due to the ablative nature of the CO_2 laser, the stratum corneum overlying the cavity was often absent (Figs. 1A,B,D and 2C). On occasion, we noted an intact stratum corneum (Figs. 1C and 2A,B,D). This is attributed to the lesions being sectioned slightly off the center axis. Within the range of pulse energies tested, interlesional epidermal and dermal tissues were found to be viable as best exemplified by positive birefringence under cross-polarized microscopy (data not shown) and LDH staining (Fig. 2).

Figures 3 and 5 represent lesion dimension plots and summarize the results of the experiments shown in Figures

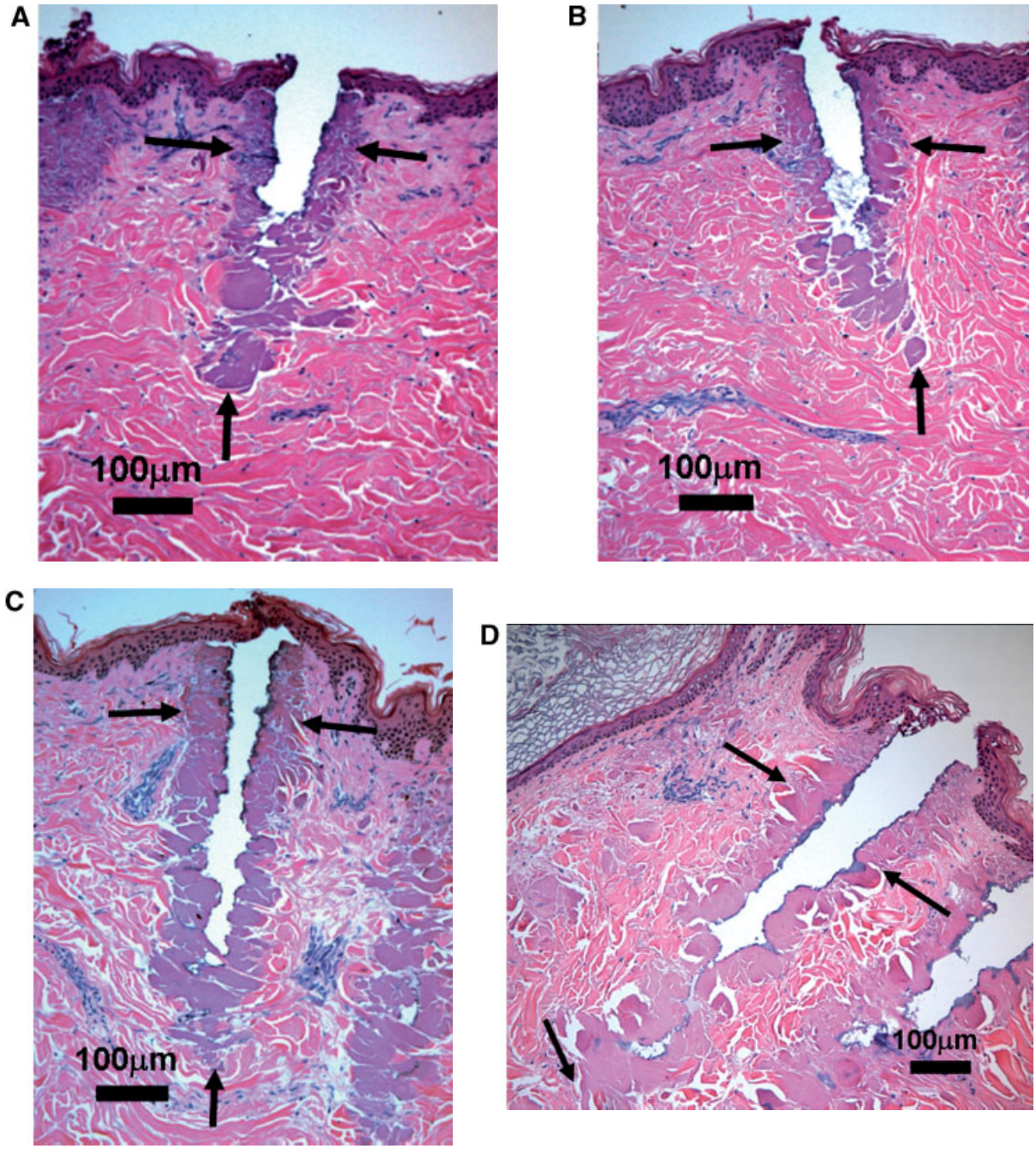

Fig. 1. Ex vivo human abdominal tissue treated with the 30 W, 10.6 μm CO_2 laser at 9.2 mJ (**A**), 13.8 mJ (**B**), 18.0 mJ (**C**), and 23.3 mJ (**D**). Paraffin embedded, H&E stained sections show tapering thermal treatment voids that are lined by a thin layer of eschar formation and surrounded by a zone of thermal coagulation representing denatured collagen. The arrows outline the extent of denatured collagen zones.

1, 2, and 4. An almost 150% increase in pulse energy from 9.2 to 23.3 mJ resulted in a $66 \pm 5\%$ increase in lesion width (Figs. 3 and 5) and a $99 \pm 6\%$ increase in lesion depth (Figs. 3 and 5). Table 1 represents a summary of lesion dimension measurements obtained after staining with LDH versus H&E at various pulse energies based on data shown in Fig. 3. We consistently detected a statistically significant ($P<0.05$) increase of approximately 10% in both mean width (ranging 8.6–18.0%) and depth (ranging 4.2–14.3%) of LDH lesions when compared to those obtained with H&E.

In a previous study, we recognized the limitation of vertical sectioning accurately locating the widest and deepest boundaries of a lesion [18]. To overcome this

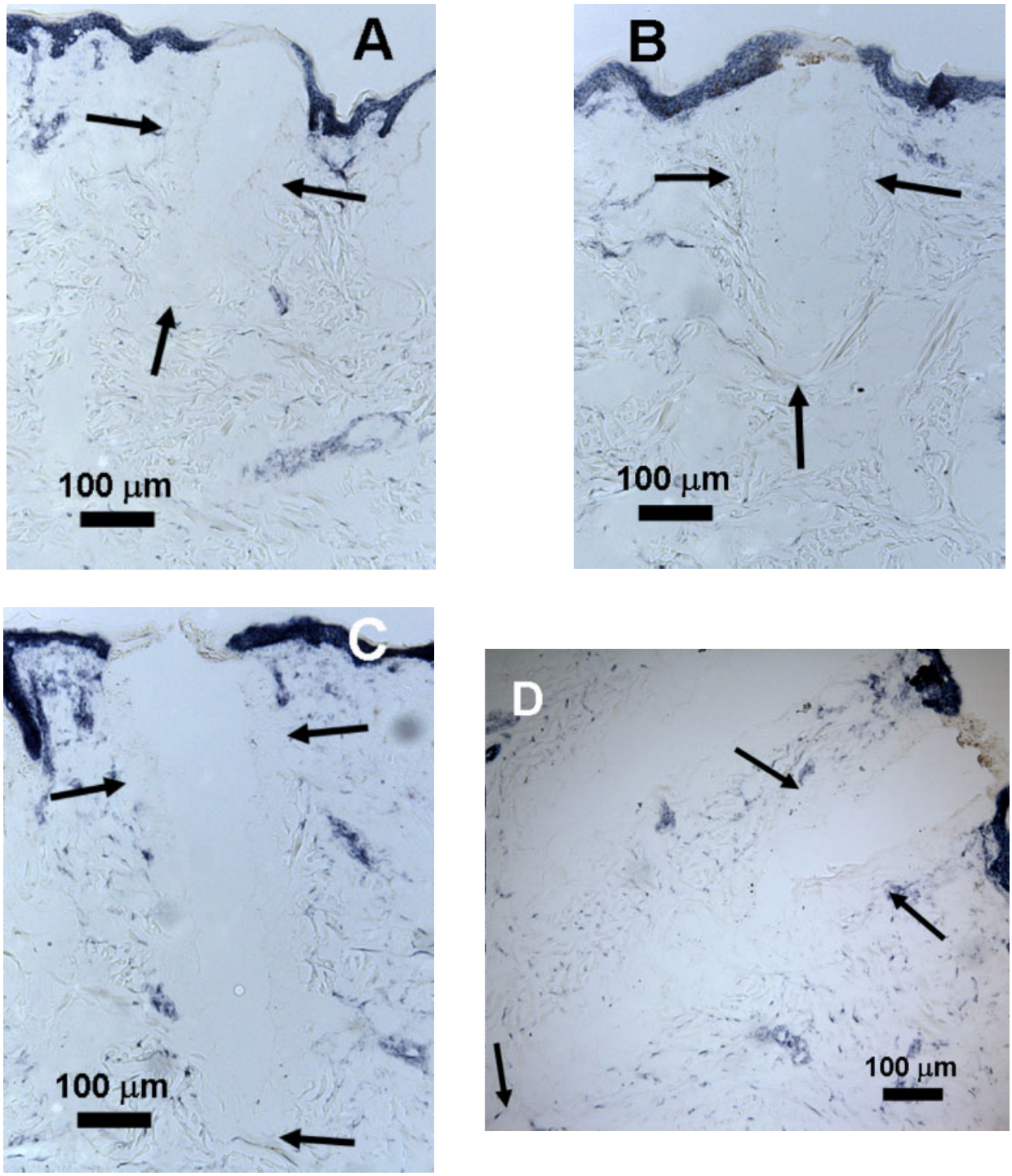

Fig. 2. Ex vivo human abdominal tissue treated with the 30 W, 10.6 μm CO_2 laser at 9.2 mJ (**A**), 13.8 mJ (**B**), 18.0 mJ (**C**), and 23.3 mJ (**D**). These samples were embedded in OCT followed by frozen sectioning and LDH staining. The presence of ablated voids is consistent with those in H&E stained samples. The arrows outline the extent of non-viable zones.

limitation, we decided to utilize a horizontal serial frozen sectioning technique that allowed visualization of the true center of each cavity thus providing a more precise estimate of lesion width. Figure 4 illustrates the results of an 18.0 mJ treatment sectioned horizontally and then stained with LDH. From an en face view, most lesions were circular in shape and characterized by a central void surrounded by an annular zone of non-viable tissue. On higher magnification,

TABLE 1. Comparison of Mean Lesion Depths and Widths for LDH and H&E Stained Samples at Selected Treatment Energies Based on Figures 1 and 2

Pulse energy (mJ)	Type of staining	Lesion depth (μm)	Student *t*-test, *P*	Lesion width (μm)	Student *t*-test, *P*
9.2	H&E	434 ± 64	0.04	193 ± 11	0.03
	LDH	475 ± 39		215 ± 18	
13.8	H&E	550 ± 51	0.01	233 ± 24	0.01
	LDH	593 ± 47		253 ± 10	
18.0	H&E	658 ± 65	0.0001	249 ± 26	0.0003
	LDH	752 ± 38		285 ± 30	
23.3	H&E	872 ± 57	0.01	317 ± 23	0.01
	LDH	909 ± 23		374 ± 32	

a thin layer of eschar formation lining the cavity wall was appreciated. Interlesional tissue clearly stained positively with LDH indicating the preservation of cellular viability in that region. Similar results were obtained at pulse energies of 9.2, 13.8, and 23.3 mJ.

Figure 5 is a reconstruction plot of the MTZ, based on the experimental data shown in Figure 4 for 9.2, 13.8, 18.0, and 23.3 mJ. As mentioned before, the en face view produced better representation of the lesion characteristic, especially at higher pulse energies where there was a higher chance of sectioning error in vertical sections that consistently underestimated the true depth of the lesions. For example, both Figures 3 and 5 showed a similar lesion depth of approximately 480 μm at 9 mJ, but the en face view produced more representative lesion depths of approximately 1 mm at 23.3 mJ (Fig. 5) compared to that with vertical section of similar pulse energy (Fig. 3).

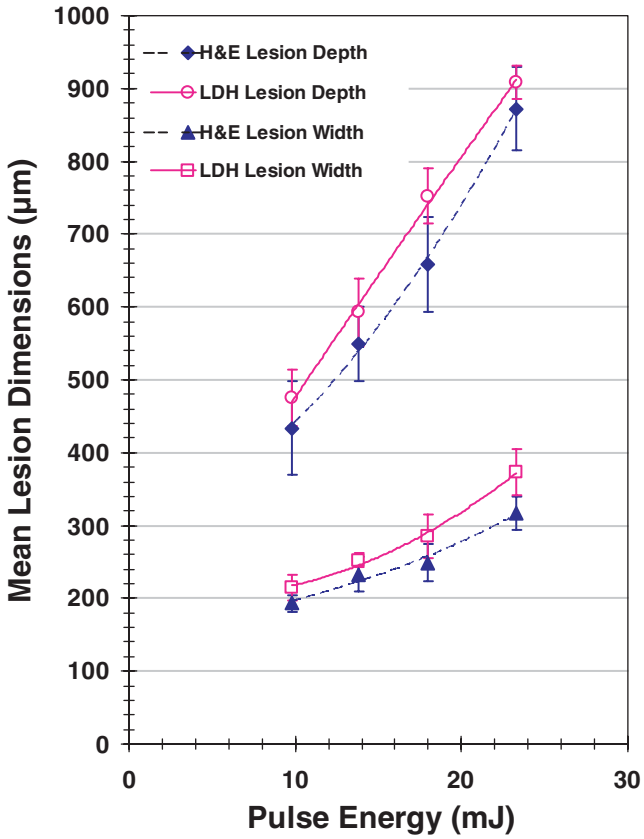

Fig. 3. Plots of mean lesion depth and width following treatment of human abdominal skin ex vivo at varying pulse energies using the fractional CO_2 laser system. Results are a plot of the average of over 200 sample measurements obtained from experiments shown in Figures 1 and 2. Note on average the larger zones of cell death (depth and width) by LDH stain versus collagen denaturation zones by H&E stain.

The lesion dimensions based on Figure 5 are tabulated in Table 2. The lesion depths/widths represent the total depths/widths of the ablation depths/widths and the cell necrotic zone. The ablation widths ranged from 103 ± 13 to 164 ± 14 μm, while the ablation depths ranged from 280 ± 10 to 760 ± 10 μm, respectively, from 9.2 to 23.3 mJ. The thicknesses of the cell death or necrotic zones, *k*, at various pulse energies were also measured. The cell necrotic zones seemed to remain around 70 μm in thickness and independent of pulse energies, except for at 23.3 mJ where the thickness increased to 92 ± 8 μm ($P<0.05$). By including both the ablative and necrotic zones, the lesion widths ranged from 233 ± 11 to 381 ± 26 μm, while the lesion depths ranged from 480 ± 10 to 1,000 ± 10 μm, respectively, from 9.2 to 23.3 mJ.

A dosimetry plot representing the surface area coverage of treatment after a varying number of passes at 400 MTZ/cm^2 is shown in Figure 6. Treatment coverage increased with increasing pulse energy, given a fixed final spot density (MTZ/cm^2) and vice versa. Beyond a treatment density of 2,400 MTZ/cm^2 at pulse energies of 14 mJ or greater, the treatment coverage seems to reach some asymptotic saturation levels.

DISCUSSION

Although ablative skin resurfacing has been in practice for over a decade now [19,20], the use of a microscopic fractional treatment approach has not yet been described. Recent advances in non-ablative treatment discovered by our group resulted in the novel concept of fractional resurfacing [12]. This mechanism of laser treatment allows for the creation of microscopic arrays of photothermal lesions in a specified portion of the overall skin. Therefore, this technique leaves a significant volume of normal healthy tissue untreated, enhancing the response

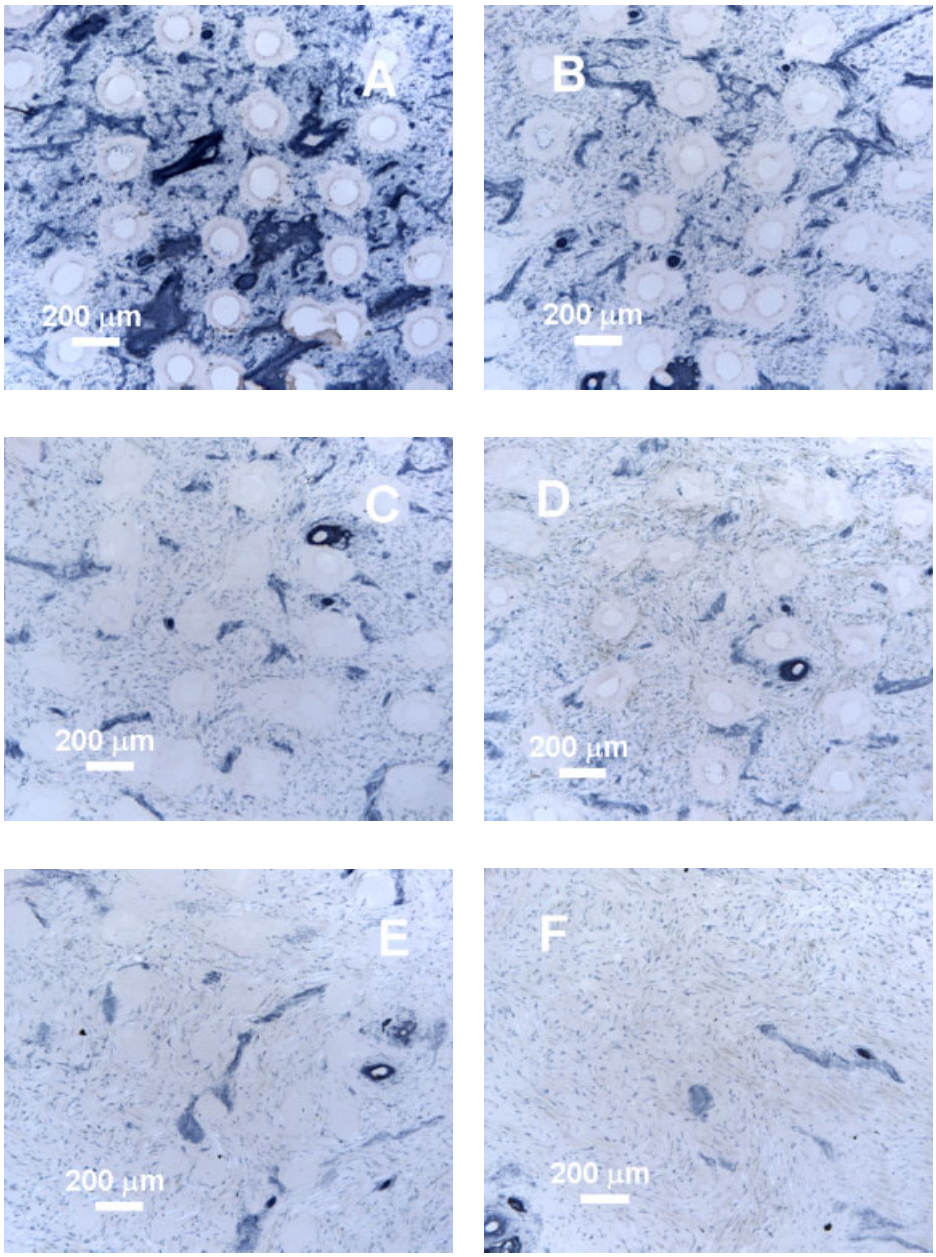

Fig. 4. Composite histology images showing en face views of an ex vivo skin sample treated with the 30 W, 10.6 μm CO_2 laser at 18.0 mJ. The frozen sectioned LDH stained sections show lesions at depths of 40 μm (**A**), 100 μm (**B**), 200 μm (**C**), 400 μm (**D**), 600 μm (**E**), and 800 μm (**F**). Serial step sections of 10 μm were taken until no further evidence of the MTZ was visualized by LDH staining. The maximum margin of error was therefore seen at 9.2 mJ (the shallowest lesions) and corresponded to less than 5%, a value less than the error between different sample measurements.

to thermal injury with more vigorous wound healing. In the current study, we sought to employ this novel approach by replacing an infrared fiber laser source with a CO_2 laser.

While nonablative fractional resurfacing sought to coagulate but not remove tissue, the novel AFR^{TM} technique drilled and removed a micro-column of epidermal and dermal tissues producing micro-lesions up to 1 mm in depth at 23.3 mJ (Fig. 5). In an unpublished study, biopsies from human forearms irradiated with the prototype device taken 1–3 months post-treatment demonstrated tissue replacement in the absence of any histological evidence of scar formation. Through preliminary histology evaluation, there is evidence that collagen has replaced the cavity in

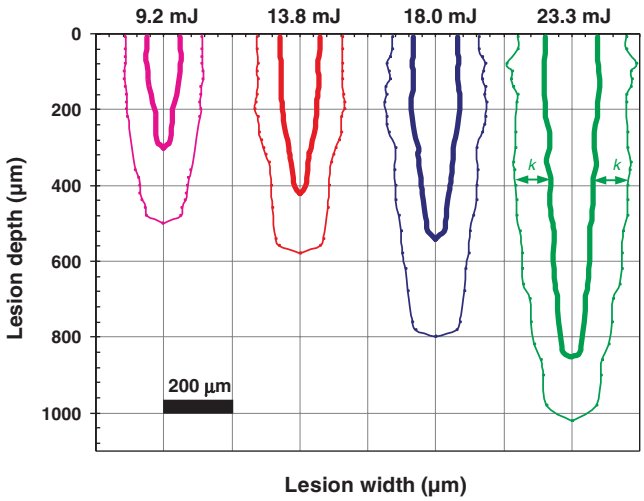

Fig. 5. Lesion reconstruction plots using measurements from serial horizontally sectioned samples treated ex vivo with the 30 W, 10.6 μm CO_2 laser at pulse energies of 9.2, 13.8, 18.0, and 23.3 mJ (from left to right). The thick and thin solid lines represent the edge of the ablated void and non-viable zone, respectively. *k* represents the thickness of the cell death or necrotic zone. The dimensions of the maximum ablation widths, maximum ablation depths, maximum lesion widths, maximum lesion depths, and cell-death zones are given in Table 2.

the ablated area. The chronological development of wound healing is currently under investigation and will be reported in a follow-up study. AFR™ introduces the possibility of tissue removal at dermal depths not previously possible with any laser modality, while may allow surgeons to overcome treatment-limiting side effects such as prolonged healing or downtime, commonly encountered after traditional ablative resurfacing performed using a non-fractional technique.

Another unique characteristic of the ablative micro-lesion is its thin layer of coagulated zone as indicated in Figure 1A–D, adjacent to the ablated zones. On each micro-lesion, there is an annular coagulated zone around the tapering ablated zone with thicknesses ranging from 40 to 75 μm, slightly narrower than the cell-death or necrotic zone that ranged from 70 to 92 μm (Figs. 2 and 4, Table 2). In the dermis, the annular coagulated zone represents denatured collagen that may provide shrinkage (discussed later) and hemostasis in vivo. Future clinical studies hope to more definitively address these benefits. We speculate that the coagulated zone of denatured dermal collagen can be ideal for minimizing bleeding—though may vary from one subject to another—while also maximizing interlesional epidermal and dermal viability that is critical for wound healing and allowing larger amount of tissue removal at higher treatment coverage with minimal downtime and long-term adverse sequelae. This is not possible with conventional CO_2 laser resurfacing, not only because the entire epidermis was removed during treatment, but also because a thicker zone of coagulated dermis up to 150 μm was produced [21,22]. The extensive thermal damage of CO_2 laser resurfacing might have interfered with optimal wound healing, resulting in significant downtime and undesirable cosmetic outcome.

We successfully created the first fractional ablative CO_2 laser capable of delivering microscopic arrays of irradiation for the treatment of human skin. By setting the spot density to 400 MTZ/cm^2, the prototype device predictably generated a pattern of ablative and thermal lesions with a pitch of approximately 500 μm. This allowed a large volume of epidermis and dermis to remain untreated. Unlike typical ablative laser treatments which generate a broad rectangular-shaped graded thermal coagulation zone parallel to the surface of the skin [23], the configuration employed in our study created multiple tapering and vertically aligned deep micro-lesions (Figs. 1, 2, and 4). We feel this is an important feature of the prototype device that allows deep dermal tissue ablation while maintaining interlesional tissue viability. Under traditional circumstances, ablative laser resurfacing treats 100% of the skin surface area, leaving only the underlying untreated dermal tissue spared from thermal damage. This can lead to a persistent textural change with an unnatural waxy appearance of the overlying treated skin.

We also attempted to better characterize the zone of ablation and thermal damage by comparing lesion dimensions obtained with LDH versus H&E staining while holding all other treatment parameters constant. Not surprisingly, our measurements using LDH were consistently larger than those obtained after H&E staining ($P<0.05$, Table 1). Thus, the total zones of cell death (LDH) were $9.0 \pm 4.2\%$ deeper and $13.2 \pm 4.0\%$ wider than zones of collagen denaturation (Fig. 3 and Table 1). This

TABLE 2. The Dimensions of Ablative Micro-Lesions Measured Based on the Lesion Reconstruction in Figure 5

Pulse energy (mJ)	Maximum ablation width (μm)	Maximum ablation depth (μm)	Maximum lesion width (μm)	Maximum lesion depth (μm)	Cell-death or necrotic zone (μm), *k*
9.2	103 ± 13	280 ± 10	233 ± 11	480 ± 10	70 ± 7
13.8	118 ± 9	480 ± 10	265 ± 29	560 ± 10	73 ± 5
18.0	143 ± 13	520 ± 10	299 ± 32	780 ± 10	72 ± 7
23.3	164 ± 14	760 ± 10	381 ± 26	$1{,}000 \pm 10$	92 ± 8

A lesion depth of more than 1 mm may be achieved at or beyond 23.3 mJ. The cell-death zones also consisting of denatured collagen may provide for hemostasis for the AFR™ modality.

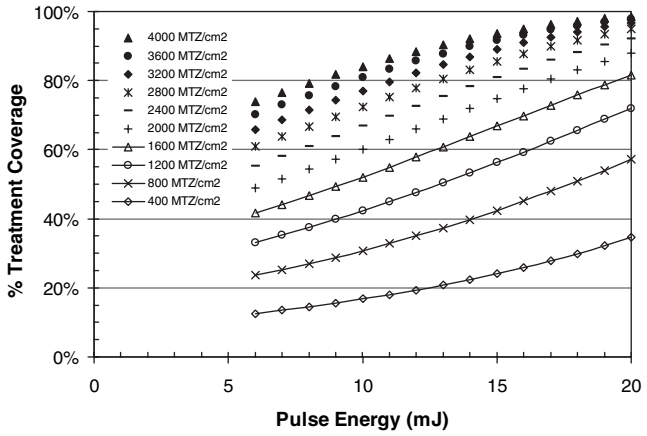

Fig. 6. Dosimetry chart of surface area coverage based on LDH measurements obtained after treatment with the prototype fractional CO_2 laser system with a 400 MTZ/cm^2/pass setting. For treatment requiring more than 400 MTZ/cm^2, multiple passes of treatment over an area are performed, resulting in the probability of micro-lesion overlap. The statistical nature of this random overlapping process was included in the computation of this dosimetry chart.

correlated to a $28.1 \pm 9.6\%$ greater cross-sectional area for cell death compared to collagen denaturation for any tested pulse energy. Although these differences appear to be relatively small, they are significant when estimating surface area coverage and volume of treated tissue for dosimetry calibration. In other unpublished work carried out by our group, we have demonstrated that cell death or necrosis was achieved at lower temperatures than collagen denaturation. Thus, the overall volume of tissue exposed to the cell necrosis threshold temperature is better assessed by LDH than H&E. We propose that LDH-based surface area measurements represent a more useful method to guide physicians on dosimetry (Fig. 6). The dosimetry chart in Figure 6 was generated based on a simple probabilistic formulation:

$$p(Q,D) = 1 - [1 - A(Q) \cdot D]^n, \quad \text{where } A(Q) \cdot D < 1 \quad (1)$$

where $p(Q,D)$ is the probabilistic treatment coverage; 1 means 100% treatment coverage, while 0 means 0% treatment coverage. Multiplying $p(Q,D)$ with 100 produces treatment coverage in percent. $A(Q)$ is the single MTZ cross-sectional area as a function of pulse energy, $Q \cdot D$ is the MTZ/cm^2/pass setting used in the treatment, and n is the number of passes performed within the same treatment area. Equation (1) implies that the treatment coverage is dependent upon the pulse energy, Q, density-per-pass setting, D, and the number of passes, n, performed. This formulation provides a reasonable estimation of the level of treatment coverage from the probabilistic standpoint due to the quasi-random nature of fractional treatment after multiple passes, accounting for overlapping of micro-lesions. Future experimental work will be performed to validate this theoretical model.

At present, the treatment coverage for optimal efficacy of any clinical indication for the AFR^{TM} modality remains unknown. We hypothesize that it may be possible that an AFR^{TM} treatment could afford higher percentage treatment coverage within a treatment session as compared to a nonablative fractional resurfacing treatment. In an AFR^{TM} treatment, the short pulse duration produced by a high power 30-W laser ablated a large volume of epidermal and dermal tissue. Because the ablation process proceeded upon irradiation, it removed a major portion of the heat generated through optical absorption along with the ejected debris, before thermal diffusion into the skin could occur. This may explain the fact that only a very thin layer of denatured collagen (Fig. 1) or necrosis (Figs. 2 and 4, Table 2) was produced with the diffusion of the residual heat. As a result, the amount of heat remaining in the tissue by an AFR^{TM} treatment may be comparatively much less than that generated by an NFR^{TM} treatment, and a subject may be able to tolerate a higher level of treatment coverage within a treatment session. Nevertheless, it is very likely the AFR^{TM} modality is suitable for clinical indications different from those of the NFR modality. Hence, it may not be fair to compare the AFR^{TM} and NFR^{TM} modalities from a simplistic view of treatment coverage. Scientific investigation and clinical studies are currently underway.

Unlike ablative CO_2 lasers, which generate tissue shrinkage or skin tightening by bulk tissue removal and coagulation, AFR^{TM} treatment may achieve the same goal through an entirely different and novel three-dimensional mechanism. We hypothesize that AFR^{TM} treatment resurfaces and removes micro-columns of tissue deep in the dermis while creating an annular zone of coagulation surrounding each cavity. The annular configuration of coagulated and tightened collagen functions as a matrix, effectively creating multiple centers of micro-contraction. These zones of radial contraction will undoubtedly affect long-term wound healing and contribute to both immediate macroscopic skin shrinkage and long-term persistence of skin tightening. We hypothesize that at a constant treatment density, the pulse energy (i.e., depth of lesion) becomes the dominant predictor of final tissue shrinkage and vice versa. Further work is currently underway to better comprehend this relationship.

Ablative CO_2 lasers have been shown to generate high-tissue temperature profiles exceeding well over 300°C [23] across the entire treatment surface. Although the presence of suprathreshold temperatures certainly generates a heat shock response, enzymatic activity is lost and structural proteins denatured forcing the wound-healing response to come from beneath the graded thermal coagulation zone. This results in prolonged healing times manifest as months of clinical erythema in patients who undergo traditional CO_2 laser resurfacing. Thus, AFR^{TM} may offer several advantages in wound healing by maintaining a significant volume of viable tissue at the macroscopic, and more critically, microscopic levels. First, the new AFR^{TM} modality having spot sizes of less than 500 μm may be optimal for rapid epidermal wound healing by minimizing the keratinocyte migration path or time period. The fractional

approach combined with optimal treatment coverage or spot density and pulse energy may allow for a favorable ratio of viable to treated tissue. When the ratio of the zone of thermal damage to viable tissue becomes unfavorable, such as in the case of conventional ablative resurfacing, key cytokines are unable to diffuse great lengths due to their limited concentration gradients as most of the signaling molecules have been destroyed during treatment. Therefore, basal-layer stem cells are not recruited and a suboptimal wound healing process results. On the other hand, AFR™ treatment may provide for an optimal wound-healing response and avoid full surface area enzymatic destruction and cell necrosis, thereby maximizing in three dimensions, the ability of normal tissue to accelerate the repair process.

In conclusion, we report for the first time the successful development of a prototype AFR™ device for the treatment of human skin. Although traditional erbium:YAG and CO_2 lasers have been hampered by the significant incidence of side effects, we believe the configuration employed in the design of this novel prototype CO_2 laser device will allow the treating physician to overcome these historical limitations. An IRB-approved multi-center full-face clinical study is currently under way, and indeed, preliminary clinical results showed promising results with no observable permanent side effects. This observation is consistent with the lack of any published reports indicating more permanent side effects using the non-ablative Fraxel® SR (NFR™) laser device. In fact, a recent report by Fisher et al. [13] demonstrated a resolution of most side effects in less than 1 week post-treatment. Future investigations will focus on further characterization of the clinical and histological features of this novel AFR™ prototype CO_2 laser.

REFERENCES

1. Ratner D, Tse Y, Marchell N, Goldman MP, Fitzpatrick RE, Fader DJ. Cutaneous laser resurfacing. J Am Acad Dermatol 1999;41:365–389.
2. Ross EV, Miller C, Meehan K, McKinlay J, Sajben P, Trafeli JP, Barnette DJ. One-pass CO_2 versus multiple-pass Er:YAG laser resurfacing in the treatment of rhytides: A comparison side-by-side study of pulsed CO_2 and Er:YAG lasers. Dermatol Surg 2001;27:709–715.
3. Manuskiatti W, Fitzpatrick RE, Goldman MP. Long-term effectiveness and side effects of carbon dioxide laser resurfacing for photoaged facial skin. J Am Acad Dermatol 1999;40:401–411.
4. Fitzpatrick RE, Goldman MP, Satur NM, Tope WD. Pulsed carbon dioxide laser resurfacing of photo-aged facial skin. Arch Dermatol 1996;132:395–402.
5. Zachary CB. Modulating the Er:YAG laser. Lasers Surg Med 2000;26:223–226.
6. Horton S, Alster TS. Preoperative and postoperative considerations for carbon dioxide laser resurfacing. Cutis 1999;64:399–406.
7. Sriprachya-Anunt S, Fitzpatrick RE, Goldman MP, Smith SR. Infections complicating pulsed carbon dioxide laser resurfacing for photoaged facial skin. Dermatol Surg 1997;23:527–536.
8. Schwartz RJ, Burns AJ, Rohrich RJ, Barton FE, Byrd HS. Long-term assessment of CO_2 facial laser resurfacing: Aesthetic results and complications. Plast Reconstr Surg 1999;103:592–601.
9. Trelles MA, Allones I, Luna R. Facial rejuvenation with a nonablative 1320 nm Nd:YAG laser: A preliminary clinical and histologic evaluation. Dermatol Surg 2001;27:111–116.
10. Menaker GM, Wrone DA, Williams RM, Moy RL. Treatment of facial rhytids with a nonablative laser: A clinical and histologic study. Dermatol Surg 1999;25:440–444.
11. Manstein D, Herron GS, Sink RK, Tanner H, Anderson RR. Fractional photothermolysis: A new concept for cutaneous remodeling using microscopic patterns of thermal injury. Lasers Surg Med 2004;34:426–438.
12. http://www.reliant-tech.com
13. Fisher GH, Geronemus RG. Short-term side effects of fractional photothermolysis. Dermatol Surg 2005;31:1245–1249.
14. Rokhsar CK, Fitzpatrick RE. The treatment of melasma with fractional photothermolysis: A pilot study. Dermatol Surg 2005;31:1645–1650.
15. Rostan EF. Laser treatment of photodamaged skin. Facial Plast Surg 2005;21:99–109.
16. Tannous ZS, Astner S. Utilizing fractional resurfacing in the treatment of therapy-resistant melasma. J Cosm Laser Ther 2005;7:39–43.
17. Fisher GH, Kim KH, Bernstein LJ, Geronemus RG. Concurrent use of a handheld forced cold air device minimizes patient discomfort during fractional photothermolysis. Dermatol Surg 2005;31:1242–1244.
18. Bedi VP, Chan KF, Sink RK, Hantash BM, Herron GS, Rahman Z, Struck SK, Zachary CB. The effects of pulse energy variations on the dimensions of microscopic thermal treatment zones in nonablative fractional resurfacing. Lasers Surg Med (in press).
19. Rosenberg GJ. New directions in laser therapy: Combination of carbon dioxide laser resurfacing and incisional cosmetic facial surgery. Clin Plast Surg 2002;29:53–79.
20. Ross EV, McKinlay JR, Anderson RR. Why does carbon dioxide resurfacing work? A review. Arch Dermatol 1999;135:444–454.
21. Fitzpatrick RE, Ruiz-Esparza J, Goldman MP. The depth of thermal necrosis using the CO_2 laser: A comparison of the superpulsed mode and conventional mode. J Dermatol Surg Oncol 1991;17:340–344.
22. Alster TS, Kauvar ANB, Geronemus RG. Histology of high-energy pulsed CO_2 laser resurfacing. Semin Cutan Med Surg 1996;15:189–193.
23. Ross EV, Yashar SS, Naseef GS, Barnette DJ, Skrobal M, Grevelink J, Anderson RR. A pilot study of in vivo immediate tissue contraction with CO_2 skin laser resurfacing in a live farm pig. Dermatol Surg 1999;25:851–856.